Implementation of the continuous wavelet transform for digital time series analysis

D. Jordan and R. W. Miksad[a)]
School of Engineering and Applied Science, University of Virginia, Charlottesville, Virginia 22903

E. J. Powers
Department of Electrical and Computer Engineering, University of Texas, Austin, Texas 78712

(Received 10 July 1996; accepted for publication 9 October 1996)

The wavelet transform has emerged as an important tool for the analysis of intermittent and nonstationary signals. This article addresses implementation issues of a digital continuous wavelet transform that is sufficiently general that any continuous wavelet can be used. Working equations are derived for wavelet sampling, aliasing, and scale population by using the band-pass filter interpretation of wavelet functions. The implementation procedure is applied to the Morlet wavelet in detail as an example. Finally, the Morlet wavelet is applied to velocity fluctuations measured in a subsonic wake undergoing transition to turbulence. © *1997 American Institute of Physics.* [S0034-6748(97)01002-2]

I. INTRODUCTION

The wavelet transform has in recent years found application in numerous fields of engineering and science. As a tool that complements the well-known Fourier analysis, it is useful for the analysis of intermittent and nonstationary signals obtained from experimental measurements. In the field of fluid mechanics, time series obtained from fluid turbulence and transition to turbulence often display intermittent fluctuations.[1,2] Decomposition of such signals with the Fourier basis is not always insightful, since the Fourier basis does not possess the property of locality inherent to these signals. Wavelets, on the other hand, are localized functions which better reflect the properties of time-dependent signals. The continuous wavelet transform decomposes a signal into a time-scale representation that elucidates the intermittent characteristics of the signal.

This article focuses on the continuous wavelet transform where the analysis in time and in scale is continuous as opposed to the orthogonal or discrete wavelet transform where the analysis occurs discretely in time and scale. There are certain advantages to using continuous wavelet analysis. For example, the band center frequency for the continuous wavelet transform can be changed continuously (up to sampling limits) when rescaling but the band center frequency of orthogonal wavelets is usually changed by a factor of 2 when rescaling. Even though it has many properties desirable for the analysis of signals,[2] less attention has been given to the digital implementation of the continuous wavelet transform than the orthogonal counterpart. Some of the major issues of implementation are discussed in Ref. 2 but these are not developed in detail. Considerable effort is required to implement a digital continuous wavelet transform from the current literature.

It is the purpose of this article to convey a procedure for implementing the continuous wavelet transform for the application of digital time series analysis. To this effect, this article addresses the major issues including sampling the wavelet and determining the scale population from the smallest to largest scales. Equations for implementation parameters are derived, relying primarily on the overlapping band-pass filter interpretation of continuous wavelet functions. Furthermore, since the wavelet transform can be performed with a number of different wavelet functions, the presentation is sufficiently general so that any continuous wavelet can be implemented. The Morlet wavelet, the most commonly used continuous wavelet, is used throughout to illustrate the implementation procedure.

The Morlet wavelet is then used to study the temporal characteristics of velocity fluctuations of a plane wake undergoing transition to turbulence. It is well documented that the velocity fluctuations in the initial stages of transition have a wave character consistent with linear theory as described by the Rayleigh equation. At large amplitude these waves undergo nonlinear interactions which energize other waves in the spectrum. Therefore, spectral (Fourier) analysis has been very successful in characterizing these stages of transition. However, it has been observed[3,4] that prior to the onset of turbulence, the velocity fluctuations from the wake exhibit irregular, intermittent behavior which is difficult to study with spectral analysis. The time-localized property of wavelet analysis offers an avenue for quantifying the intermittent aspects of transition. Measurements of the u' velocity fluctuation in a subsonic wake are analyzed with the wavelet transform as an illustration of wavelet analysis in a practical application.

II. COMPLEX-VALUED CONTINUOUS WAVELETS

The key feature that a continuous function, real or complex, must possess to be considered a wavelet is *admissibility*. This entails the existence of a finite constant computed from a function $\psi(t)$ which guarantees that once a function $f(t)$ is transformed to the wavelet domain, it can be recovered by applying the inverse wavelet transform. If the constant does exist and is finite, then $\psi(t)$ is a wavelet. Usually,

[a)]Dean.

 0034-6748/97/68(3)/1484/11/$10.00

the expression for the admissibility constant C_ψ is given in terms of $\hat{\psi}(\omega)$, the Fourier transform of $\psi(t)$. In this article, the definition of the Fourier transform is

$$\hat{\psi}(\omega)=\frac{1}{2\pi}\int_{-\infty}^{\infty}\psi(t)\exp(-i\omega t)dt, \tag{1}$$

which gives the resulting expression for the admissibility constant,

$$C_\psi=2\pi\int_{-\infty}^{\infty}|\hat{\psi}(\omega)|^2\frac{d\omega}{\omega}. \tag{2}$$

Next, the $\mathscr{L}^2$ inner product is defined as

$$\langle f,g\rangle=\int_{-\infty}^{\infty}fg^*dt, \tag{3}$$

where $*$ denotes the complex conjugate. It can be shown[5,6] that for finite energy functions, i.e., $\langle\psi,\psi\rangle<\infty$, which have a continuous Fourier transform, the admissibility condition simplifies to

$$\int_{-\infty}^{\infty}\psi(t)dt=0. \tag{4}$$

Therefore, admissibility requires the function to be nonzero only on a finite extent of the time axis and to oscillate with zero mean in order to be classified as a wavelet. Thus, the familiar sine and cosine functions are excluded from this definition of wavelets because they oscillate with zero mean but are infinite in extent.

This article deals with complex-valued wavelets which generate wavelet coefficients expressible as a magnitude and a phase. An example of a complex-valued wavelet is the Morlet wavelet whose real and imaginary parts are shown in Fig. 1. The expression for the Morlet wavelet in the time domain is given as

$$\psi(t)=\exp(i\omega_\psi t)\exp(-|t|^2/2), \tag{5}$$

where $\omega_\psi\epsilon[5,6]$ is a constant that forces the admissibility condition to be satisfied. The wavelet function so defined is termed the *mother wavelet*. All other wavelets used in the analysis are translations and dilations of the mother wavelet,

$$\psi_{a,\tau}=a^{-1/2}\psi\left(\frac{t-\tau}{a}\right), \tag{6}$$

where the factor $a^{-1/2}$ is a normalization which gives all dilated versions of the mother wavelet the same energy. Note that the scale parameter a is nondimensional and is the ratio of the support (size) of the dilated wavelet to the support of the mother wavelet.

Applying the Fourier transform defined in Eq. (1) gives the Morlet wavelet in the frequency domain,

$$\hat{\psi}(\omega)=\begin{cases}(2\pi)^{-1/2}\exp-(\omega-\omega_\psi)^2/2, & \omega>0\\ 0, & \omega\leqslant 0\end{cases}, \tag{7}$$

which can be viewed as a band pass filter. Also, applying the Fourier transform to Eq. (6) gives

$$\hat{\psi}_{a,\tau}(\omega)=a^{1/2}\hat{\psi}(a\omega)\exp(-i\omega\tau). \tag{8}$$

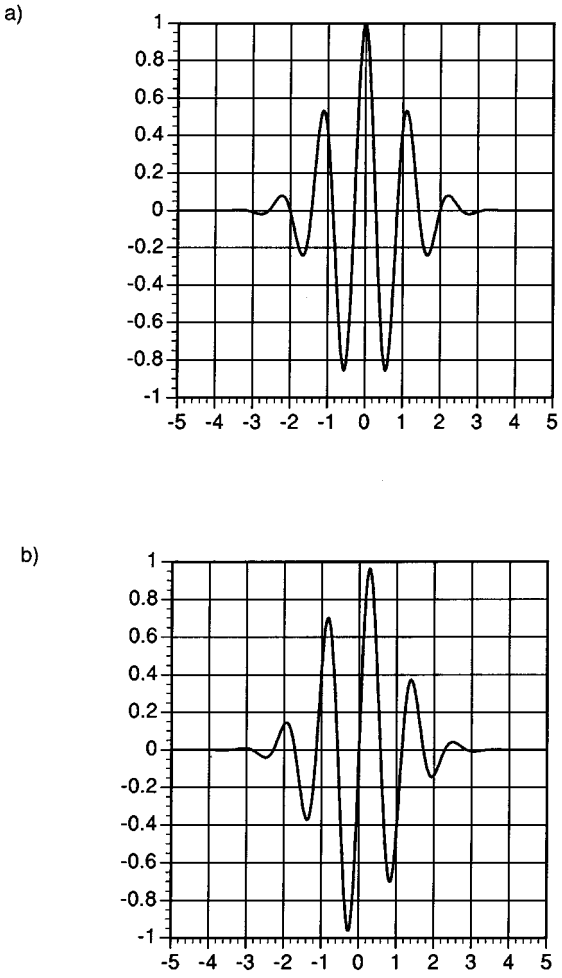

FIG. 1. Complex-valued Morlet wavelet: (a) real part; (b) imaginary part.

In the frequency domain, dilated and translated wavelets result in a series of ''constant Q'' band-pass filters. The magnitude of the Fourier transform of two scaled versions of the Morlet wavelet is shown in Fig. 2.

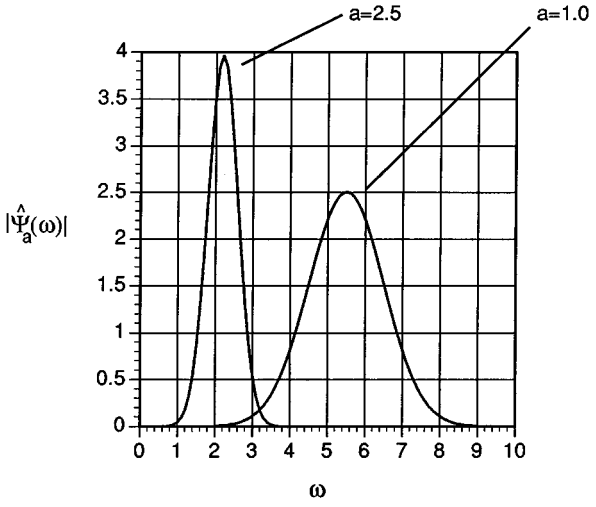

FIG. 2. Frequency domain representation of the Morlet wavelet. An increase in wavelet scale, a, corresponds to a decrease in the center frequency.

III. NUMERICAL ALGORITHM FOR THE CONTINUOUS WAVELET TRANSFORM

The wavelet transform of a function is the projection of that function onto all scaled (dilated) and translated versions of a single mother wavelet having the properties defined in the previous section. In function space, such as $\mathscr{L}^2$ space, the projection is accomplished through an inner product integral. This is not a new concept since the Fourier transform is computed in exactly the same manner by projecting a function onto the complex exponential basis, $\exp(-i\omega t)$. Mathematically, the wavelet transform is expressed

$$\mathscr{W}(a,\tau)=\langle f(t),\psi_{a,\tau}\rangle=\int_{-\infty}^{\infty} f(t)\psi^*_{a,\tau}(t)dt, \tag{9}$$

where again

$$\psi_{a,\tau}=a^{-1/2}\psi\left(\frac{t-\tau}{a}\right) \tag{10}$$

describes all scaled and translated versions of the mother wavelet. Combining Eqs. (9) and (10) yields

$$\mathscr{W}(a,\tau)=a^{-1/2}\int_{-\infty}^{\infty} f(t)\psi^*\left(\frac{t-\tau}{a}\right)dt. \tag{11}$$

Because of the shifting property of the transform (the presence of $-\tau$), the wavelet transform of a function at a given scale is a convolution integral between the function of interest and the wavelet function at the given scale. Therefore the basic algorithm for computing the wavelet transform is a set of convolution integrals parametrized by the scale, a. Convolutions are usually performed in the frequency domain to take advantage of the simplicity (multiplications) and efficiency of convolution in Fourier space. The diagram in Fig. 3 illustrates the general procedure for performing the digital continuous wavelet transform.

IV. BACKGROUND CALCULATIONS

When implementing continuous wavelet analysis, it is good practice to make several preliminary calculations. Each of these calculations is an integral over time or frequency which is most easily evaluated numerically. The first set of calculations deals with admissibility. If, as in most cases, the proposed wavelet has finite energy, then one need only to check that the zero mean condition is satisfied by evaluating Eq. (4). In the case of the Morlet wavelet, however, the integral in (4) gives a small nonzero result that takes on its minimum magnitude when the parameter $\omega_\psi\epsilon[5,6]$. The value of the Morlet mean when $\omega_\psi=5.5$, used for the Morlet wavelet in this article, is calculated to be $-0.000\,106$ which is on the order of the numerical error in the wavelet transform calculation as discussed in Ref. 2. The admissibility constant itself should also be calculated from Eq. (2) since it is usually involved in expressions dealing with the wavelet energy density and the inverse wavelet transform.[2,5,7]

The next set of calculations characterize the properties of the time and frequency windows of the mother wavelet. These are the center (first moment) and the standard deviation (second moment) of the time and frequency windows[5,7]

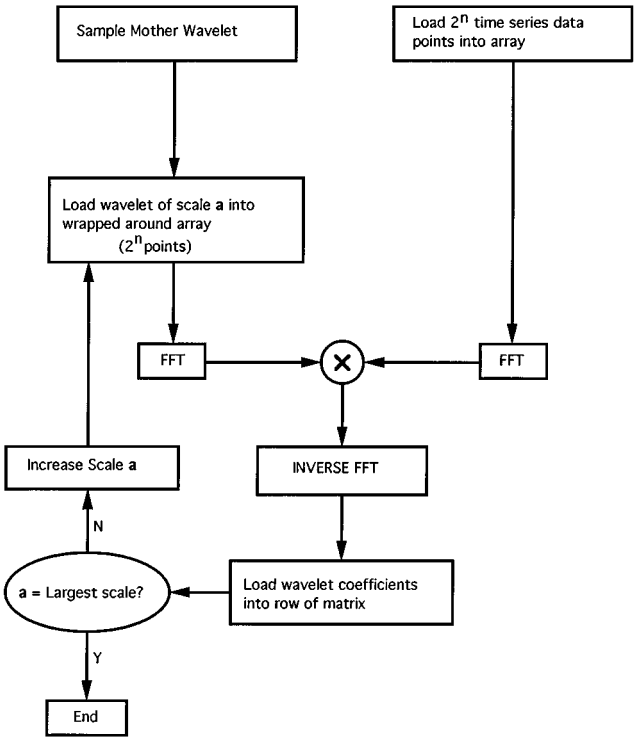

FIG. 3. Diagram of digital continuous wavelet transform algorithm.

$$t_0=\frac{\int_{-\infty}^{\infty} t|\psi(t)|^2\,dt}{\int_{-\infty}^{\infty}|\psi(t)|^2\,dt}, \tag{12}$$

$$\sigma_t=\left(\int_{-\infty}^{\infty}(t-t_0)^2|\psi(t)|^2\,dt\right)^{1/2}, \tag{13}$$

$$\omega_0=\frac{\int_{-\infty}^{\infty}\omega|\psi(\omega)|^2\,d\omega}{\int_{-\infty}^{\infty}|\psi(\omega)|^2\,d\omega}, \tag{14}$$

$$\sigma_\omega=\left(\int_{-\infty}^{\infty}(\omega-\omega_0)^2|\psi(\omega)|^2 d\omega\right)^{1/2}. \tag{15}$$

Table I summarizes the Morlet wavelet parameters computed with numerical integration.

V. WAVELET SAMPLING

A. Dimensional expressions

In order to use the framework of continuous wavelets to analyze discretely sampled data, it is necessary to sample the analyzing wavelet. In sampling the wavelet there is an inherent clipping of the end at a time denoted T. Hence window decay will stop at time locations given by $-T$ and T for symmetric wavelets and locations given by t_0-T and t_0+T for nonsymmetric wavelets. One method for choosing the

TABLE I. Morlet wavelet parameters, $\omega_\psi=5.5$.

t_0	0.0
σ_t	0.941 396
ω_0	5.5
σ_ω	0.375 007
C_ψ	0.327 835

cutoff endpoints is to set the value of T equal to $3\sigma_t$. Furthermore, it is also good practice to sample the wavelet to preserve symmetry. For example, the Morlet wavelet can be sampled on an odd number of points by taking the center point and an even number of points out to T on each side of the center. The utility of this method is demonstrated by noting that convolution with a delta function gives back the function centered at the location of the delta function. Sampling in this manner preserves this convolution property in the digital implementation. For larger scale sampling the value of $\psi(T)$ is computed from the mother wavelet and then the sample cutoff value is $a^{-1/2}\psi(T)$, consistent with the chosen normalization, to give the same percent of amplitude cutoff at each scale.

Some important relations can be derived from the wavelet equations with simple manipulations. First, however, it must be realized that the sampling time of the wavelet, Δt, does not correspond to the sampling time of the physical quantity, $\Delta t'$, to be analyzed since the wavelet time base is nondimensional. This is simple to reconcile if the following approach is used.

The relationship between the dimensional and nondimensional sampling times can be obtained through the number of sample points of the wavelet. Consider the physical time series sampled with sampling time $\Delta t'$ seconds. The total amount of dimensional time for N points which will be defined as the number of points the wavelet is sampled on is $N\Delta t'$. Therefore if the total nondimensional time is $2T$ then the mapping for N points (see Fig. 4) is

$$[-T,T]\leftrightarrow[0,N\Delta t']. \tag{16}$$

To convert the equations defining the wavelets from the nondimensional to the dimensional domain then the one simply uses

$$t=\frac{2T}{N\Delta t'}\,t', \tag{17}$$

where $'$ denotes a dimensional quantity.

Similarly, the equations for the frequency content of the wavelets are written in nondimensional form. These can be converted to dimensional form in the same way by noting that the units for frequency in Hz is s^{-1}. This leads to an analogous expression for frequency after substituting $\omega=2\pi f$,

$$f=\frac{N\Delta t'}{2T}\,f'. \tag{18}$$

In summary, to convert wavelet expressions for dimensional use

$$\psi(t)=\psi\left(\frac{2T}{N\Delta t'}\,t'\right), \tag{19}$$

$$\hat{\psi}(f\ )=\hat{\psi}\left(\frac{N\Delta t'}{2T}\,f'\right). \tag{20}$$

The usefulness of such expressions is demonstrated with the Morlet wavelet. First note the general form of the Morlet wavelet equations after the conversion defined in Eqs. (19) and (20):

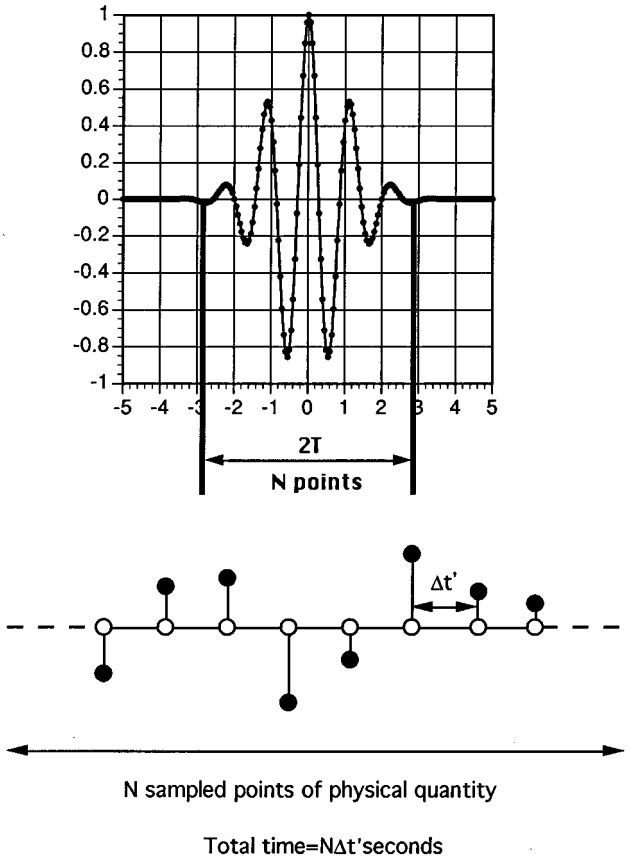

FIG. 4. Correspondance between sampled points of the physical quantity and the sampled points of the wavelet.

$$\psi_{a,\tau'}(t')=a^{-1/2}\exp\left(\frac{i2\omega_\psi T}{aN\Delta t'}\,(t'-\tau')\right)\times\exp\left(-\left|\frac{2T}{aN\Delta t'}\,(t'-\tau')\right|^2\Big/2\right), \tag{21}$$

$$\hat{\psi}_{a,\tau'}(f')=\left(\frac{a}{2\pi}\right)^{1/2}\exp\left[-\left(\frac{\pi a f' N\Delta t'}{T}-\omega_\psi\right)^2\Big/2\right]\times\exp\left(\frac{-ia\pi f' N\Delta t'\tau'}{T}\right). \tag{22}$$

Each scaled version of the wavelet corresponds to a bandpass filter with a translated band peak along the frequency axis. From these dimensional equations we can extract a direct relationship of the scale, a, and its band peak frequency, f_p', in units of Hz, invaluable for interpreting results. In general, the expression for the band peak frequency can be derived by taking the derivative of the magnitude of the filter function and setting it equal to zero. For the Morlet wavelet, though, note that the filter takes on it's peak value when the argument of the exponential is zero. So in this case,

$$\frac{\pi N\Delta t' f_p'}{T}-\omega_\psi=0. \tag{23}$$

Hence, the peak frequency for a given scale in the Morlet wavelet is defined as

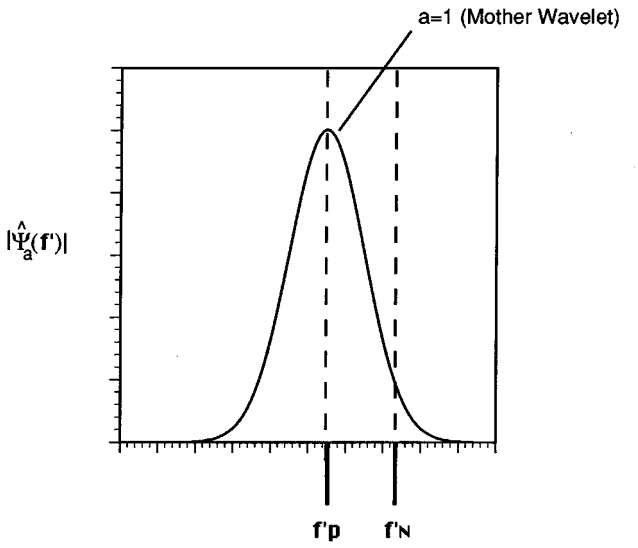

FIG. 5. The Nyquist criterion and mother wavelet aliasing.

$$f'_p = \frac{T\omega_\psi}{\pi \Delta t' N a}. \tag{24}$$

Note that the expression depends upon the number of data points the mother wavelet is sampled on as well as the sampling interval of the experimental time series. For a given set of sampled data the largest peak frequency is determined by the number of sample points of the *mother wavelet*. With less sample points the largest peak frequency can be increased but only up to a limit determined by the aliasing effects. An expression is derived next to show the minimum number of points required to avoid aliasing.

B. Aliasing considerations

The Nyquist criterion describes how to avoid aliasing when a fluctuation is being sampled: *The highest frequency that will not be aliased is equal to half the sampling frequency*, $f_s/2$. The wavelet mother function can also be aliased if there are not enough samples, i.e., too small of a sampling frequency. By considering the frequency content of the mother wavelet and the Nyquist frequency of the time series, an expression is derived for the minimum number of sample points for the wavelet. Choose the highest band peak frequency such that the band pass filter magnitude decays to acceptably small values at the Nyquist frequency as illustrated in Fig. 5. This guarantees that the entire frequency band of the mother wavelet is less than the Nyquist frequency. Since all larger scales have band-pass filters centered at a lower frequency than the mother wavelet, they meet the Nyquist criterion as well. The percent of decay from the largest peak frequency is defined as

$$\eta = \frac{|\hat{\psi}_{a=1,\tau'}(f'_N)|}{|\hat{\psi}_{a=1,\tau'}(f'_p)|} \tag{25}$$

with $a=1$ representing the mother wavelet.

This calculation will be illustrated with the Morlet wavelet. Substituting Eq. (22) for the expression for $\hat{\psi}_{a,\tau'}$ and noting that $f'_N = 1/2\Delta t'$ at the Nyquist frequency

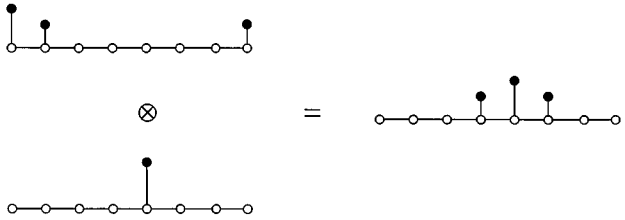

FIG. 6. Illustration of convolution of a delta function with a wrapped-around filter-like function.

$$\eta = \exp\left[-\left(\frac{\pi N}{2T} - \omega_\psi \right)^2 \Big/ 2 \right]. \tag{26}$$

Finally,

$$N = \frac{2T}{\pi} \left(\omega_\psi + \sqrt{-2 \ln \eta} \right) \tag{27}$$

which is the minimum number of points on which the *Morlet* wavelet should be sampled.

C. Array loading

Another consideration is how to load the sampled wavelet into the calculation array. First, use 2^n points for both the time series array and the sampled wavelet array where n is an integer to facilitate the use of the fast Fourier transform (FFT) for convolutions. As discussed earlier, a useful sampling of the wavelet is an odd number of points which includes the center of symmetry. Load the sampled mother wavelet in wrap-around form by placing the center sample in the first array location. $(N-1)/2$ more samples are loaded in the beginning of the array and the remaining $(N-1)/2$ samples are loaded in wrap-around order at the end of the array. Zeros fill in the rest of the array. With an increase of the scale, a, the process is the same except the scaled wavelet array will have less points set to zero. Figure 6 illustrates such an array loading and the resulting digital convolution with a delta function as discussed in Ref. 8.

VI. SCALE POPULATION

Aliasing determines the size of the smallest scale by which all other scales are measured. Theoretically, all such scales are to be computed in the wavelet transform. However, for digital implementation the number of scales is determined by the number of points of the time series and resolution requirements.

A. Largest scale

Mathematically, the continuous wavelet transform includes all scales over the range $[0^+,\infty)$. From a signal analysis point of view, the computed scales should include those of physical interest in the signal. However there is also a practical upper limit of scale which depends on the number of points in the time series to be analyzed.

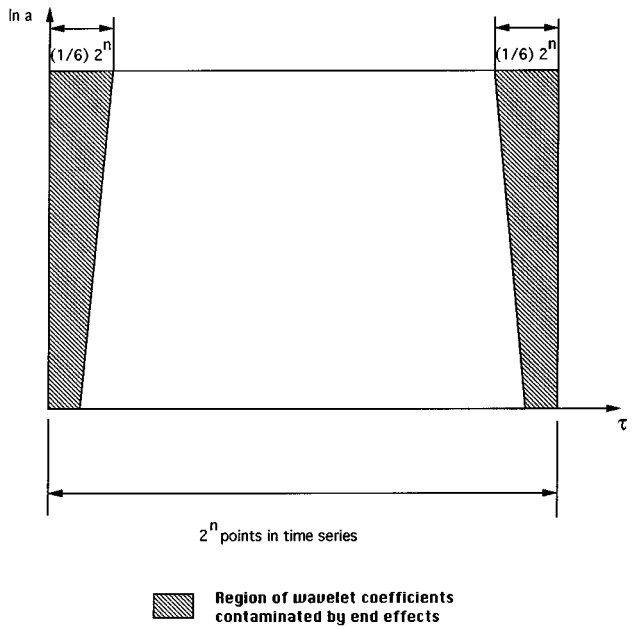

FIG. 7. Convolution end effects in the time-scale plane of wavelet coefficient plots.

To understand this concept, consider the process of discrete convolution when the time series has a finite number of points. When a convolution at a sample point is calculated, the shifted function is centered at that sample and the value of the convolution depends upon contributions from points before and after the sample point. It is clear that points near the end cannot represent the true discrete convolution between the time series and function. In fact when using the FFT to perform convolution, the convolved points near the ends include contributions that are located at the opposite end of the time series. In this discussion these points will be termed *wrap-around points*. Furthermore, as the scale increases, the number of wavelet samples to each side of the wavelet center also increases so that the number of wrap-around points increases with the scale. These points do not represent the true wavelet coefficients and should not be used in subsequent analysis. With large enough scale, all of the computed wavelet coefficients are wrap-around points.

The number of wrap-around points can be determined as a function of scale. Based on an odd number of wavelet samples, the number of points that are wrapped around *at each end of the time series* is equal to the number of points sampled on each side of the center sample of the wavelet. Since the number of wavelet function sample points scales with a, an estimate of the number of wrap-around points at one end for a scale is given by

$$N_w(a) \approx \frac{a(N-1)}{2}. \tag{28}$$

Since the wrap-around points are generally not useful for analysis, a large-scale cut-off criterion needs to be prescribed. There is a trade off in computing larger scales and only having a small fraction of the large scale coefficients unaffected by the ends (see Fig. 7). It is desirable that the useful large scale coefficients are a sizable fraction of the length of the time series. Otherwise only a few coefficients in the center of the time axis will be meaningful. The compromise used in this work is to make the largest scale equal to the scale where 1/3 of the coefficients are affected by the ends. This criterion is implemented by taking the ratio of the number of wrap-around points at the largest scale to the total number of points in the time series and prescribing it to be less than or equal to 1/6. [Note that the number of wrap-around points in Eq. (28) is for one end of the plot.] This gives

$$\frac{a_{\max}(N-1)/2}{2^n} \leqslant \frac{1}{6}. \tag{29}$$

Of course, the criterion of 1/6 is rather arbitrary and it is up to the judgement of the individual to determine a suitable criterion for a given application. Solving for the exponent, n, gives

$$n \geqslant \frac{\ln[3a_{\max}(N-1)]}{\ln 2}. \tag{30}$$

Conversely, if the length of the time series is fixed then the largest scale that should be analyzed based on the above criterion is

$$a_{\max} \leqslant \frac{2^n}{3(N-1)}. \tag{31}$$

These expressions are useful for determining the size of the time series required to obtain useful wavelet coefficients in the scale range of interest.

B. Resolution

The continuous wavelet transform prescribes a continuous distribution of wavelet coefficient scales to be computed. However, for digital implementation, only discrete values of scale need to be computed. This section addresses how to populate the discrete scales and gives a method for populating with a given scale resolution. Resolution is an important issue because the resolution requirements change depending upon the content of the signal. For example, one would use a much different resolution for a signal with frequencies from 1 to 1000 Hz than for a signal with frequencies from 1 Hz to 10^{10} Hz. Furthermore, there is a trade-off in resolution and storage space. Every scale that is computed generates the same number of wavelet coefficients as there are points in the time series. The total number of wavelet coefficients is the number of scales multiplied by the number of time series points. Obviously the number of coefficients and the storage space directly depends upon the resolution.

The constant $\Delta f/f$ property of the wavelet band-pass filters implies that the bandwidth decreases as the corresponding scale increases as shown in Fig. 2. A constant spacing of band-pass filters would not sufficiently cover the low frequency region or would require such a high resolution that it would inefficiently overpopulate the high frequency range. Therefore, to accomplish sufficient coverage in the frequency domain efficiently, the spacing of consecutive band-pass filters should decrease as the scale increases. To obtain the

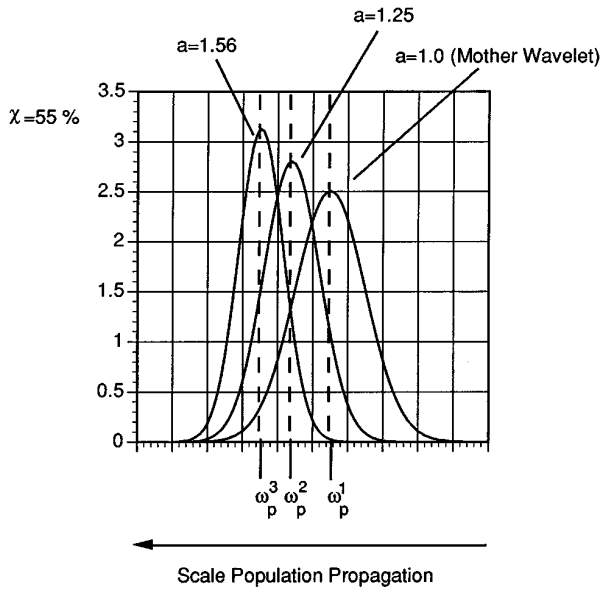

FIG. 8. Scale population procedure with $\chi=0.55$ for the Morlet wavelet.

desired result, the spacing of consecutive band-pass filters is made proportional to the inverse of the scale. For convenience, each band-pass filter is denoted by the location of its peak frequency. In other words,

$$\Delta\omega_p \propto \frac{1}{a}. \tag{32}$$

If the scales are indexed by i with $i=1$ being the smallest scale (mother wavelet) then the above expression can be written as

$$\omega_p^{i+1}-\omega_p^i=\frac{\omega_d}{a^i}, \tag{33}$$

where the proportionality constant, ω_d, is to be determined by the scale resolution chosen for the analysis. If populating discrete scales propagates from high frequency bands to low frequency bands then one method of determining the resolution constant, ω_d, is to place the next band frequency at a specified percent of decay of the previous band-pass filter. This method is illustrated in Fig. 8.

First, a parameter is defined to control resolution. Let χ be the percent of amplitude decay of a given filter where the peak of the next filter will be located. If the next filter peaks at frequency ω_p^{i+1}, then

$$\chi=\frac{\hat{\psi}(a^i\omega_p^{i+1})}{\hat{\psi}(a^i\omega_p^i)}. \tag{34}$$

The parameter χ is in the numerical range (0.0, 1.0). Values of χ near 1.0 define a high resolution calculation while values near 0.0 define a low resolution calculation. Next, an equation will be derived that adjusts the spacing of filters for a given wavelet function based on the value of χ alone. Combining Eqs. (33) and (34) gives

$$\hat{\psi}(a^i\omega_p^i+\omega_d)=\chi\hat{\psi}(a^i\omega_p^i) \tag{35}$$

from which the value of ω_d can be determined either analytically or by numerical means. In the case of the Morlet wavelet, ω_d can be solved for analytically,

$$\omega_d=-\sqrt{-2\ln\chi}. \tag{36}$$

Note from Eq. (8) that when dilating from the mother wavelet to a scaled version that

$$\hat{\psi}(\omega)\rightarrow\hat{\psi}(a\omega). \tag{37}$$

Hence, at the band peak frequency for every scale, the value of the *argument* of ψ is a constant which equals ω_p^1. Since the value of the argument is $a\omega$ for wavelet band-pass filters, the following expression holds for each scale at the band peak,

$$\omega_p^i=\frac{\omega_p^1}{a^i}. \tag{38}$$

Equations (33) and (38) are combined to get

$$\frac{\omega_p^1}{a^{i+1}}-\frac{\omega_p^1}{a^i}=\frac{\omega_d}{a^i}, \tag{39}$$

which can be manipulated to yield the form

$$a^{i+1}=Ka^i, \tag{40}$$

where

$$K=\frac{\omega_p^1}{\omega_d+\omega_p^1}. \tag{41}$$

Once in this form note that all successive wavelet scales depend upon all previous scales such that

$$a^i=K^{(i-1)}, \tag{42}$$

where i is an integer index of the number of scales used, $a^1=1$ and $(i-1)$ is not a superscript but a power of K. With χ chosen by the user, this equation can be used in the computational algorithm to increase the wavelet scale after each discrete convolution is performed. Finally, a useful expression is obtained by solving for i,

$$i=\frac{\ln a^i}{\ln K}+1. \tag{43}$$

By using the value of $a_{\max}$ for a^i in the above expression, one can calculate the total number of scales (after rounding) required to compute up to the largest scale, $a_{\max}$, under the chosen population resolution.

VII. TESTING THE ALGORITHM

The best test that one can perform for initial testing of the implementation is to take the wavelet transform of a delta function.[2] Convolution of a function with a delta function gives back the original function centered at the location of the delta function. A correct result would give the amplitude and phase of the wavelet function at every scale.[2] If the test time series is assumed to be sampled at a rate in dimensional units then expression (21) can be used to calculate results independently to check that the amplitude and phase are correct. For example, with the Morlet wavelet, the dimensional amplitude expression is

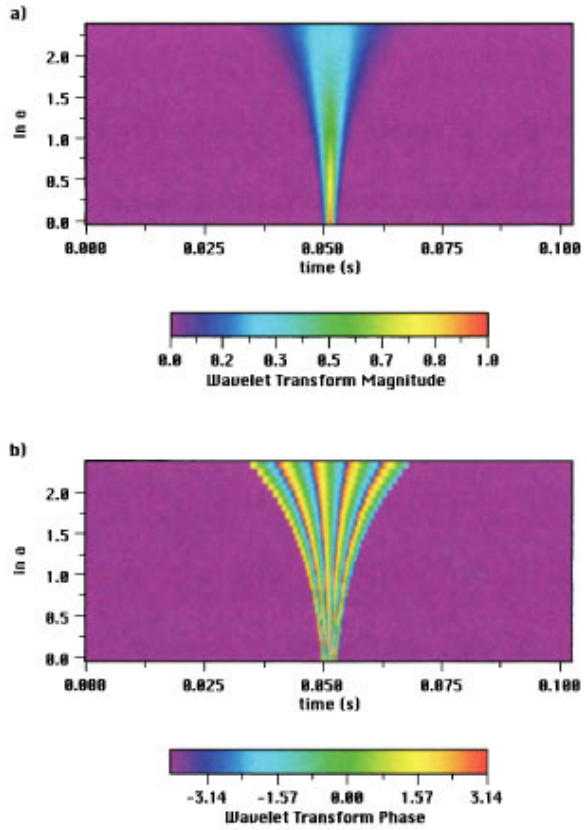

FIG. 9. Plots of the wavelet coefficients for a delta function test signal: (a) magnitude, (b) phase.

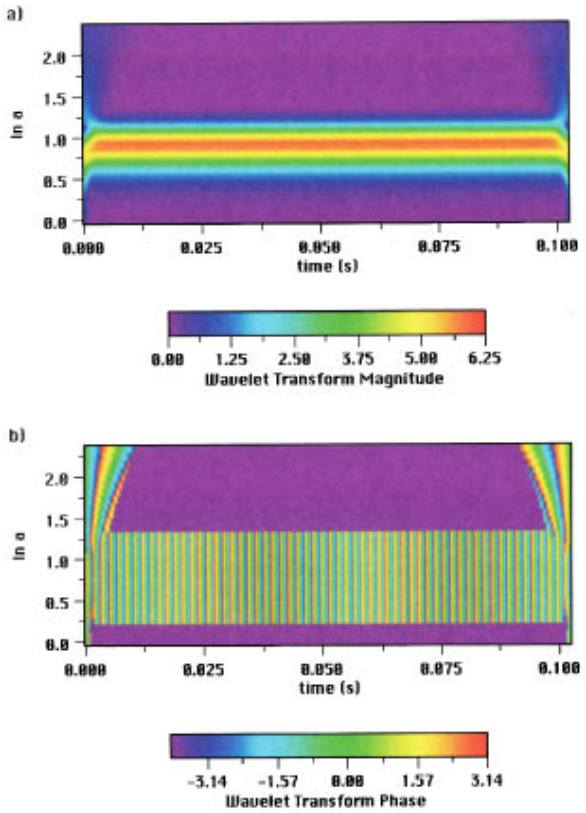

FIG. 10. Plots of the wavelet coefficients for a sampled sine wave test function: (a) magnitude, (b) phase.

$$a^{-1/2}\exp\left(-\left|\frac{2T}{aN\Delta t'}(t'-\tau')\right|^2\Big/2\right), \tag{44}$$

and the dimensional phase expression can be shown to be

$$\phi=-\frac{2\omega_\psi T}{aN\Delta t'}(t'-\tau'), \tag{45}$$

which is actually the negative of the phase of the Morlet wavelet because of the complex conjugation that appears in Eq. (3). In this equation, t' represents the location of the Morlet wavelet on the time axis. Note that when calculating the phase, the values need to be adjusted between 0 and 2π or between $-\pi$ and π. The delta function test signal with the magnitude and phase of its wavelet coefficients is shown in Fig. 9. The sampling time is 0.0002 s.

If the transform of the delta function is shown to be correct, then another common test is to use pure sinusoids of various frequencies. The magnitude of the wavelet coefficients should show a peak at the scale which has a band peak closest to the frequency of the sine wave. The phase of the coefficients should vary over 2π with each cycle of the sine wave[2] except, of course, near the ends. Plots of the wavelet coefficients for a 587 Hz sine wave of unit amplitude with a sampling time of 0.0002 s are shown in Fig. 10. The frequency, $f_p'=587$ Hz, corresponds to $\ln a=0.905$. Note that the end effects and reasons for needing to account for them show up quite clearly in these plots.

VIII. PLOTTING THE WAVELET COEFFICIENTS

Results from the continuous wavelet transform are most easily visualized in the form of color contour plots using a commercial package. One of the best methods for displaying the coefficients is to use the natural log of the scale rather than the scale itself for that axis of the plot.[2] Furthermore, the values of phase are independent of the magnitude of the coefficients and are present even if the magnitude is insignificant. Therefore it is useful to specify a threshold magnitude above which the phase is plotted and below which is the background color. This is done for the phase plots shown in Figs. 9 and 10. In Fig. 10, the phase of the coefficients is present even where the magnitude has decayed to the background, illustrating the usefulness of defining a magnitude threshold for phase plots.

IX. APPLICATION: TRANSITION TO TURBULENCE IN A SUBSONIC WAKE

A. Experimental facility and measurements

Experiments were conducted in an open return wind tunnel. The test section measures 120 cm by 20 cm by 20 cm (l-w-h). Turbulence in the ambient environment is damped by a stilling chamber with screens and with a 20:1 contraction ratio from the inlet to the test section. A sonic throat located between the test section and wind tunnel pump isolates the pump acoustic disturbances from the test section. A symmetric airfoil, designed to eliminate bluff body shedding, was placed parallel to the incoming flow near the test section entrance. The airfoil measures 20.1 cm long with a maxi-

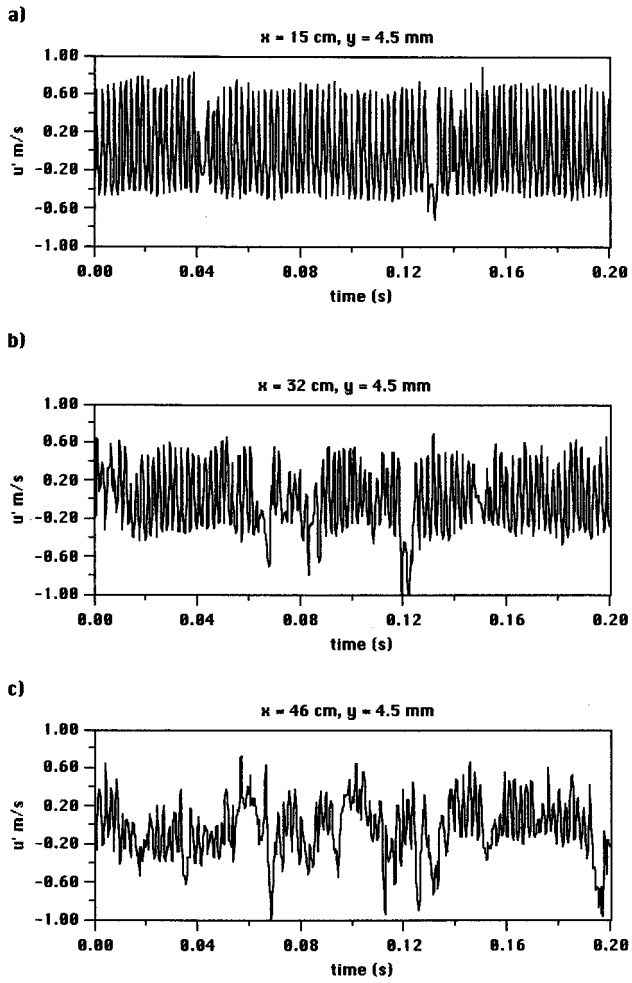

FIG. 11. u' velocity fluctuations measured in a subsonic wake: (a) $x=15$ cm, $y=4.5$ mm, (b) $x=32$ cm, $y=4.5$ mm, (c) $x=46$ cm, $y=4.5$ mm.

mum thickness of 0.31 cm and a trailing edge thickness of 0.05 cm. The origin of the coordinate system ($x=0.0$, $y=0.0$) is located at the trailing edge of the airfoil.

Measurements of the u' fluctuation were made with an Auspex u' hot-wire anemometer probe, 5.0 μm in diameter and 0.8 mm long. The hot-wire electronics included a DISA 56C17 CTA Bridge module installed in a DISA 56B01 main frame. Out of tunnel calibration was performed with a TSI model 1125 calibrator and a Dwyer model No. 400 manometer. A curve fit of the calibration curve was performed with a fourth order polynomial. The hot-wire signal was sampled and digitized with an eight channel LeCroy Camac model 8212A/8 data logger and a LeCroy CAMAC model 8800A memory module at a sampling rate of 5000 Hz.

The freestream turbulence intensity ($x=0.0$ cm, $y=20.0$ mm) was measured to be 0.079%. The freestream mean velocity was measured to be 6.7 m/s. The transition process occurred ''naturally'' from the amplification of the background fluctuations in the flow and without acoustic excitation. The naturally excited fundamental instability frequency was 430 Hz.

Examples of u' time series for three streamwise locations are shown in Fig. 11. At $x=15$ cm, the fluctuation is essentially a combination of the fundamental mode and intermittent ''events'' reminiscent of previous measurements in plane wake transition.[3,4] At $x=32$ cm the fundamental is still present but with the appearance of more intermittent events. By $x=46$ cm, the fundamental mode is quite ''patchy'' with a variety of intermittent large scale fluctuations. Note that spectral analysis can only reflect these time dependent properties of the signal indirectly. A localized fluctuation is projected onto many Fourier modes in spectral analysis making it difficult, if not impossible, to analyze the characteristics of these fluctuations. However, these intermittent fluctuations can be examined with the continuous wavelet transform.

B. Implementation of wavelet analysis

Using the methods outlined in the previous sections, the Morlet wavelet will be used to analyze velocity fluctuations obtained from the experiment. For the Morlet wavelet, $T=3\sigma_t\approx 2.82$ from Table I. The aliasing parameter, η, is chosen to be 0.01 so that only 1% of the mother wavelet is aliased.

The minimum number of points to sample is calculated first. Using Eq. (27) for the Morlet wavelet, the chosen value of η gives $N=15.32$. Choosing the next highest odd integer gives $N=17$ points. Once the value of N is determined, Eq. (24) is used to get the relationship between the peak frequency and scale,

$$f_p'=\frac{1452}{a}. \tag{46}$$

It is desired to analyze scales corresponding to frequency band peaks down to about 30 Hz. The previous equation is used to calculate the largest scale required

$$a_{\max}=\frac{1452\ \text{Hz}}{30\ \text{Hz}}\approx 48.4. \tag{47}$$

With the largest scale determined it is possible to calculate the length of the time series required to satisfy the end effect criterion. Applying the end effect criterion stated in Eq. (30), the exponent of 2 for the number of time series points is computed to be $n\geqslant 11.27$. The value of n is chosen to be 12 to give a total of 4096 points in the time series to be analyzed.

The next consideration is the scale resolution. For fluctuations where the frequency range is small it seems reasonable to use do a high resolution calculation. For this application, the scale resolution is chosen to be $\chi=0.9$. Since the calculations are being done with the Morlet wavelet, Eq. (36) can be used to compute the scale resolution parameter

$$\omega_d=-\sqrt{-2\ln(0.9)}=-0.4590. \tag{48}$$

For the Morlet wavelet band peak,

$$\omega_p^1=\omega_\psi=5.5, \tag{49}$$

which gives

$$K=\frac{5.5}{5.5-0.5701}=1.091. \tag{50}$$

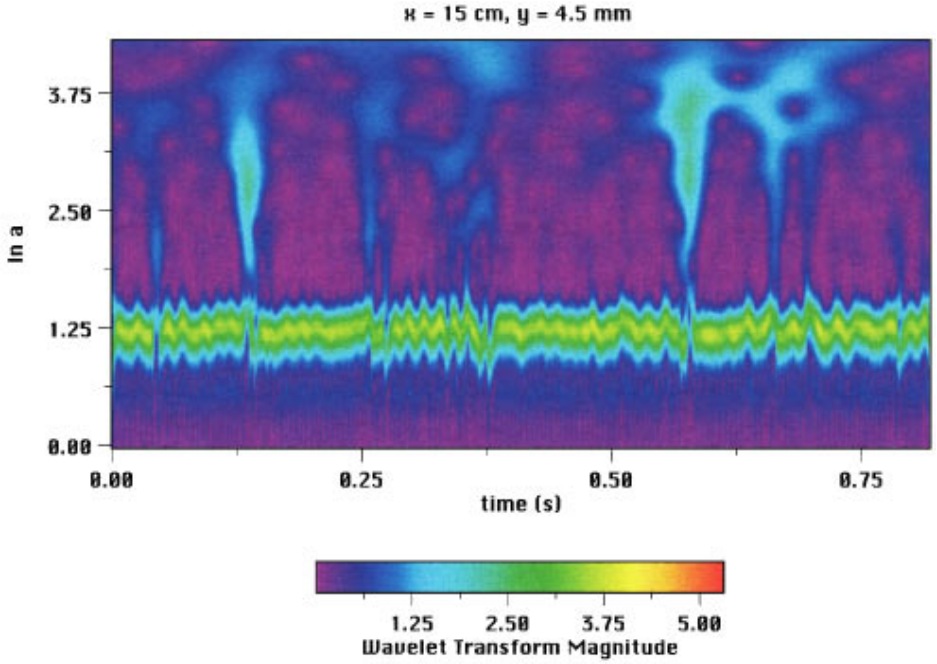

FIG. 12. Magnitude of wavelet coefficients. $x=15$ cm, $y=4.5$ mm.

From K, the total number of scales can be computed with Eq. (43),

$$i_{\max}=\frac{\ln(48.4)}{\ln(1.091)}+1=45.54\approx 46. \tag{51}$$

This gives a wavelet coefficient matrix of 46 by 4096 complex coefficients. Finally, the amount of time involved with wrap-around points at the largest scale is

$$a_{\max}\frac{N-1}{2}\Delta t'=0.077\,44\ \text{s}. \tag{52}$$

C. Results from wavelet analysis

Figures 12–14 show the magnitude of the wavelet coefficients for the fluctuations shown in Fig. 11 but over a larger time period. These plots reveal a complex visual image compared to the simple test plots in Figs. 9 and 10. They can be interpreted in the following way. Wavelet coefficients are nonzero if there is a fluctuation at the given scale (frequency band) in the associated time window. If there is no fluctuation at that scale in the time window then the coefficient is

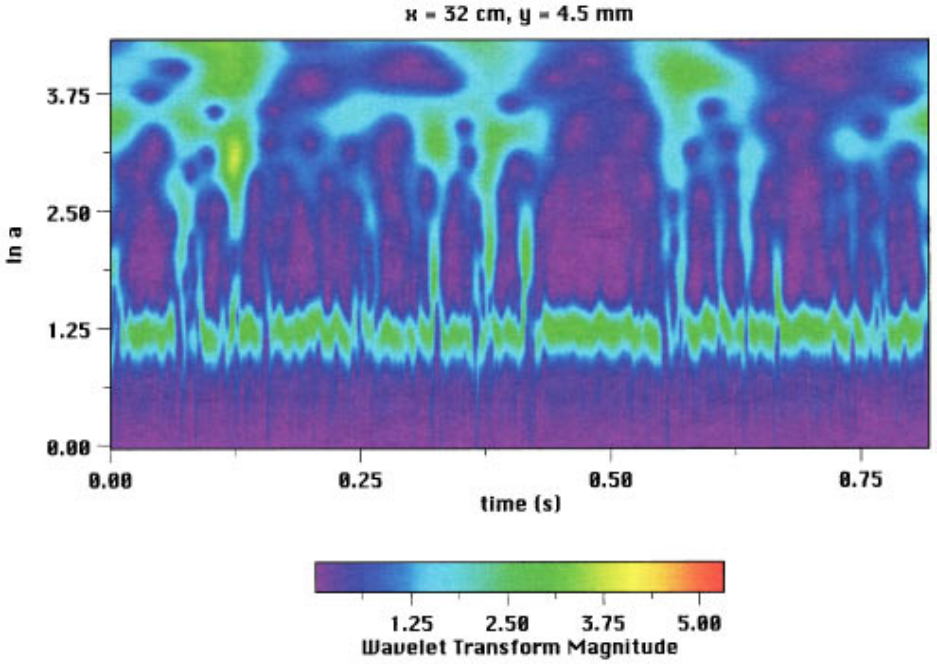

FIG. 13. Magnitude of wavelet coefficients. $x=32$ cm, $y=4.5$ mm.

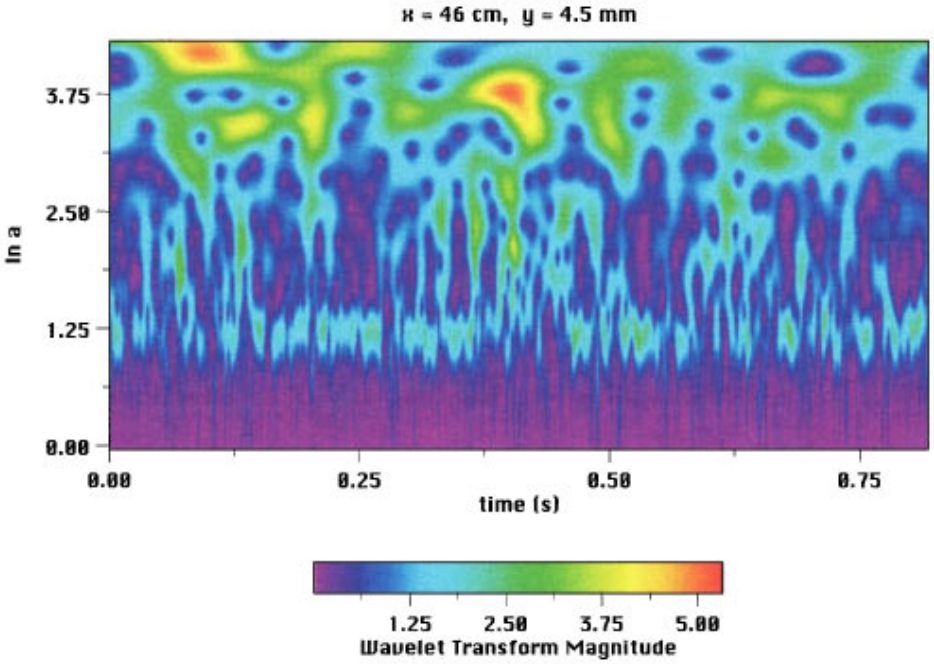

FIG. 14. Magnitude of wavelet coefficients. $x=46$ cm, $y=4.5$ mm.

zero. In this analysis, the fundamental fluctuation of 430 Hz appears at the scale, $\ln a=1.216$.

In Fig. 12, at $x=15$ cm, note that the coefficients which correspond to the fundamental do not form constant color contours in time as with the pure sinusoidal test signal. In particular, note the waviness of the coefficients from 0.25 to 0.375 s. This behavior of the coefficients is indicative of a *localized* modulation of the fundamental mode, i.e., a periodic change in frequency reflected here as a periodic change in scale. Also note that the events that appeared in Fig. 11(a) are represented as large scale localized fluctuations in the wavelet coefficients. For example, the time series in Fig. 11(a) show events centered at 0.04 and 0.013 s. Each is a highly localized event in time which will project onto many frequency bands (recall the delta function, Fig. 9) but note that there are differences between these in the wavelet coefficients. In particular, the event at 0.13 s shows a strong peak at $\ln a=2.81$ which corresponds to a filter peak of 87 Hz. There is no such peak for the event at 0.04 s.

At $x=32$ cm the scale of the fundamental shows locations where the coefficients dip to zero. Large scale fluctuations are centered about $\ln a=3.125$ which corresponds to about 63 Hz. Observe that there is a wider range of frequency bands excited over various times than there are in Fig. 12.

Finally, at $x=46$ cm there are more scales energized and the fundamental is very ''patchy'' with only a few cycles occurring at a time. Most of the scale activity is centered on the large scales between $\ln a=2.8$ and $\ln a=4.0$. Furthermore, scales in this range have a larger magnitude than the same scales in the previous plots.

Wavelet coefficients reveal several features of transition. The streamwise trend shows that an increasing number of scales are energized and the fundamental mode becomes increasingly ''patchy.'' Whereas the initial stages are dominated by the fundamental mode, the latter stages of transition become dominated by large scale localized fluctuations with frequency content less than 100 Hz. These large scale fluctuations do not appear as waves but as isolated pulses in time. The ''patchy'' coefficients of the fundamental suggest that the vortex structure of the initial instability breaks down locally. It appears that the final stages of transition can be well characterized by the scale content of localized fluctuations. These results illustrate the utility of wavelet analysis since it is clear that such observations could not be obtained from spectral analysis.

ACKNOWLEDGMENTS

The authors would like to thank Arun Bokde and Dave Weggel for many helpful comments and suggestions in the preparation of this article.

[1] J. Liandrat and F. Moret-Bailly, Eur. J. Mech. B/Fluids **9**, 1 (1990).
[2] M. Farge, Annu. Rev. Fluid Mech. **24**, 395 (1992).
[3] H. Sato and H. Saito, J. Fluid Mech. **67**, 539 (1975).
[4] R. W. Miksad, F. L. Jones, and E. J. Powers, in *Laminar-Turbulent Transition, IUTAM Symposium Novosibirsk, USSR*, edited by V. V. Kozlov (Springer, Berlin, 1984), pp. 397–409.
[5] C. K. Chui, *Wavelet Analysis and its Applications, Vol. 1: An Introduction to Wavelets* (Academic, New York, 1992), pp. 7–10.
[6] G. Kaiser, *A Friendly Guide to Wavelets* (Birkhauser, Boston, 1994), p. 70.
[7] P. Kumar and E. Foufoula-Georgiou, in *Wavelet Analysis and its Applications, Vol. 4: Wavelets in Geophysics*, edited by E. Foufoula-Georgiou and P. Kumar (Academic, New York, 1994), pp. 1–43.
[8] W. H. Press, B. P. Flannery, S. A. Teukolsky, and W. T. Vetterling, *Numerical Recipes: The Art of Scientific Computing* (Cambridge University Press, Cambridge, 1986), p. 409.